Fast Resistive Reconnection Regime in the Nonlinear Evolution of Double Tearing Modes

Z. X. Wang,[1] X. G. Wang,[2,*] J. Q. Dong,[3,4] Y. A. Lei,[2] Y. X. Long,[3] Z. Z. Mou,[3] and W. X. Qu[3]

[1]*State Key Lab of Materials Modifications by Beams, School of Physics and Optoelectronic Technology, Dalian University of Technology, Dalian, China 116024*

[2]*School of Physics, Peking University, Beijing, China 100871*

[3]*Southwestern Institute of Physics, P.O. Box 432, Chengdu, China 610041*

[4]*Institute for Fusion Theory and Simulation, Zhejiang University, Hangzhou, China 310027*

(Received 12 January 2007; published 2 November 2007)

Phases of nonlinear double tearing modes are studied numerically. The first two phases lead to the formation and growth of magnetic islands and are followed by a fast reconnection phase to complete the process, driven by a process of neighboring magnetic separatrices merging and magnetic islands coupling. The fast growth can be understood as a result of the island interaction equivalent to a steadily inward flux boundary driven. Resistivity dependences for various phases are studied and shown by scaling analysis for the first time. It is found that after an early Sweet-Parker phase with a $\eta^{1/2}$-scale, a slow nonlinear phase in a Rutherford regime with a η^{1}-scale is followed by the fast reconnection phase with a $\eta^{1/5}$-scale.

DOI: 10.1103/PhysRevLett.99.185004 PACS numbers: 52.35.Vd, 52.55.Tn, 52.65.Kj

Magnetic reconnection induced by resistive tearing modes plays crucial roles in solar and laboratory plasmas as the magnetic energy converts to kinetic energy and sometimes causes violent plasma instabilities in the process [1–4]. Multiple current layers are often formed in various solar and astrophysical plasmas [5–11], as well as in magnetic confinement configurations with a reversed magnetic shear, or nonmonotonic profile of the safety factor q, desirable for high performances and steady state operations of advanced tokamaks [12–14]. It is well known that such systems are subject to double, triple, or even multiple tearing modes (DTM [9,15–25], TTM [5,6,26,27], or MTM [11]). One of the necessary conditions for the DTM to develop is that the distance between the two resonant surfaces has to be close enough to get the modes coupled. Otherwise, two ordinary tearing modes (OTM) would develop even if the configurations had reversed magnetic shear regions [15,21,23]. The linear growth rate of DTM induced by plasma resistivity and/or anomalous electron viscosity has a scaling different from and usually, except for $m/n = 1/1$ mode, higher than that of the corresponding OTMs [15,21,27]. Similar conditions and results can also apply to TTMs and MTMs [5,11].

In comparison with the numerical simulation results, experiments showed that the nonlinear evolution of the $m/n = 2/1$ DTM led to off-axis sawteeth observed in the Tokamak Fusion Test Reactor (TFTR) [14]. Also recently, a structure driven nonlinear double tearing instability for the $m/n = 3/1$ mode in tokamak plasmas was studied [23–25]. It was pointed out that the magnetic islands initially located at the inner and outer resonant surfaces exchanged their radial positions with each other, accompanying an abrupt growth of the instability. The mechanisms for the instability were identified to be the triangular deformation of the magnetic islands and the resultant intense current point around the x point in a simulation study [23–25]. Hence, the typical structure of the deformed magnetic configuration was claimed to be the crucial element driving the instability.

In Ref. [14], however, a similar simulation for the $m/n = 2/1$ mode responsible for the off-axis sawtooth crashes found four distinguishable phases in agreement with the experiment, the early growth phase, the slow nonlinear reconnection phase, the sawtooth phase, and the final profile flatten phase. At the early growth and slow nonlinear reconnection, the islands on different resonant surfaces were well separated. In the sawtooth phase, however, the inner islands moved outward through the X points of the outer islands, while the outer islands moved inward through the X points of the inner islands, with a reconnection rate much faster than that in the Rutherford regime [28]. Clearly, the multiregime feature of the reconnection process was quite similar to those in the $m/n = 3/1$ mode simulation [23–25]. Nevertheless, due to the geometry of $m/n = 2/1$ mode, there is clearly neither triangular deformation of the magnetic island nor the intensive point-current that was thought to be responsible for the fast reconnection regime. Furthermore, the model has been also applied to solar plasmas. A numerical study for solar flares and coronal mass ejection found a similar fast reconnection regime due to island interaction but triangular deformation [9]. Therefore, the cause for the fast reconnection regime is still in question. Also, the resistivity dependence of the reconnection rate in the fast reconnection regime is not clear yet.

In this Letter, we revisit the nonlinear developments of double tearing modes in a numerical study to address the issue of how to understand the multiregime feature of the DTM, as well as the scaling of reconnection rates in various phases. In the numerical simulation, after an early phase of Sweet-Parker regime reconnection, two phases of nonlinear magnetic reconnection are revealed with a slow

Rutherford regime reconnection phase followed by a $\eta^{1/5}$ scale fast reconnection phase. And the fast growth of the instability is shown resulting from the neighboring magnetic separatrix merging and equivalent inward flux driven, which has been found in the late nonlinear development of forced reconnection [29]. Also, a general rule in predicting the final state of multiple-resonant-surface reconnection is summarized. These results can have significant impacts on magnetic fusion and solar plasma studies.

A typical two-dimensional slab with a scale length L_0 in the x direction and two layers of current flowing oppositely along the z direction embedded in a standard sheared magnetic field is applied, whereas no equilibrium flows. The magnetic field is approximated as $\mathbf{B} = B_T\hat{z} + \nabla \times (\psi\hat{z})$ with $\psi(x, y)$ the magnetic flux given in Refs. [21,22]. And with $q_s = m/n$ the safety factor on the double resonance surfaces, and R_0 the major radius of the device, we can choose an a on the order of the minor radius to satisfy $B_T = \frac{m}{n}\frac{R_0}{a}B_0$, where B_0 is the asymptotic poloidal field. The two-dimensional (or reduced) resistive magnetohydrodynamics (MHD) equations can then be written in dimensionless forms

$$\frac{\partial \rho}{\partial t} = -\mathbf{u} \cdot \nabla\rho - \rho\nabla \cdot \mathbf{u}, \tag{1}$$

$$\frac{\partial P}{\partial t} = -\mathbf{u} \cdot \nabla P - \gamma P\nabla \cdot \mathbf{u}, \tag{2}$$

$$\frac{\partial \mathbf{u}}{\partial t} = -\mathbf{u} \cdot \nabla\mathbf{u} - \frac{1}{2\rho}\nabla[\beta P + B^2] + \frac{1}{\rho}[\mathbf{B} \cdot \nabla\mathbf{B} + \nu\nabla^2\mathbf{u}], \tag{3}$$

$$\frac{\partial \psi}{\partial t} = -\mathbf{u} \cdot \nabla\psi + \eta\nabla^2\psi. \tag{4}$$

The density ρ, plasma pressure P, lengths x and y, magnetic field $\mathbf{B}$, magnetic flux ψ, plasma velocity $\mathbf{u}$, and time t are scaled by ρ_0, P_0, L_0, B_0, $\psi_0 = B_0L_0$, $u_A = B_0/\sqrt{4\pi\rho_0}$, and $\tau_A = L_0/u_A$, respectively. Also, γ is the adiabatic index. The dimensionless viscosity ν and resistivity η are normalized as $\nu = \nu_m/(u_AL_0\rho_0)$ and $\eta = \eta_m/(u_AL_0)$ with ν_m and η_m being the plasma viscosity and resistivity, respectively, and $\beta = P_0/(B_0^2/8\pi)$ being the poloidal plasma beta. The real time scale is then characterized by the Alfven time $\tau_A = L_0/u_A$, where for tokamak plasmas $L_0 \sim r_s$, with r_s the poloidal radius of the surface at $x = 0$. For the typical experiment parameters such as on TFTR sited in Ref. [14], τ_A is on the order of 0.1–1 microseconds.

The equilibrium magnetic configuration applied is the same as that in Ref. [21], with two resonant surfaces at $x = \pm x_s = \pm 0.25$. A small initial perturbation of the magnetic field is applied to the current layers of the $m/n = 3/1$ mode with the aspect ratio of $R_0/a = 5$. The numerical simulations are performed using a massively parallel code. The simulation box is $-1 \le x \le 1$, $0 \le y \le 2$, and periodic and free boundary conditions are imposed at $y = 0, 2$, and $x = \pm 1$, respectively. A Runge-Kutta finite difference scheme is used to solve the set of Eqs. (1)–(4), with fourth-order accuracy in time and second-order accuracy in space. The spatial step length is chosen to satisfy $\Delta x \ll \sqrt{\eta}$ and the temporal step length Δt is small enough to keep the numerical accuracy and stability. The convergence of the code was ensured by varying grid number and time step size. The parameters are set as $\gamma = 5/3$, $\beta = 0.5$, and $\nu = 0.2\eta$ for a given η value, such that the viscosity effect is negligible.

The time evolution of the plasma kinetic energy is given in Fig. 1 for plasma resistivity $\eta = 5 \times 10^{-5}$. Clearly, after a short linear growth, the kinetic energy goes through four developing stages as seen in the TFTR experiment [14]: the early growth, transition, fast growth, and decay. It is shown that the growths of the kinetic energy in the first two phases may be fitted with scales as η^α for the early growth and η^1 for the transition phase, respectively. The numerical scaling on resistivity in the three growth regimes are presented in Fig. 2. Clearly, as resistivity deceases, α changes from 1/2 to 1.

In previous studies, it was found that DTMs had features of non constant-ψ reconnection [15,23]. Theories for non constant-ψ reconnection have shown that after a $\eta^{1/3}$ scale linear stage, there is a $\eta^{1/2}$ early nonlinear reconnection of Sweet-Parker regime [15,30,31]. The Sweet-Parker phase is then followed by a slow Rutherford regime [32]. When the resistivity is very small, however, the DTM system degenerates into a two-OTM system despite the distance between the resonant surfaces being unchanged [15]. In such cases, the Rutherford regime directly follows the linear regime [28]. Clearly, the results are in a good agreement with the theories.

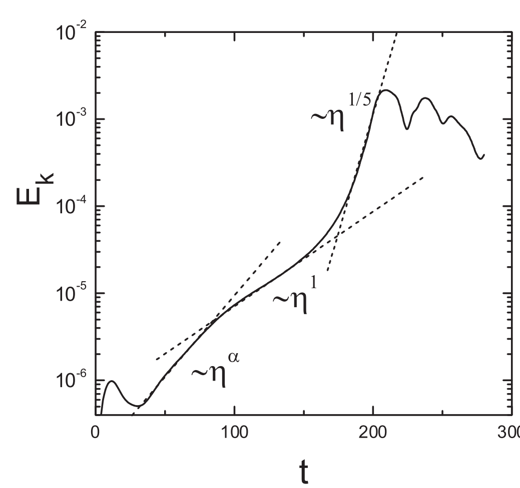

FIG. 1. Time evolution of the plasma kinetic energy $E_k = \frac{1}{2} \times \iint \rho u^2 dxdy$ for a plasma resistivity of $\eta = 5.0 \times 10^{-5}$.

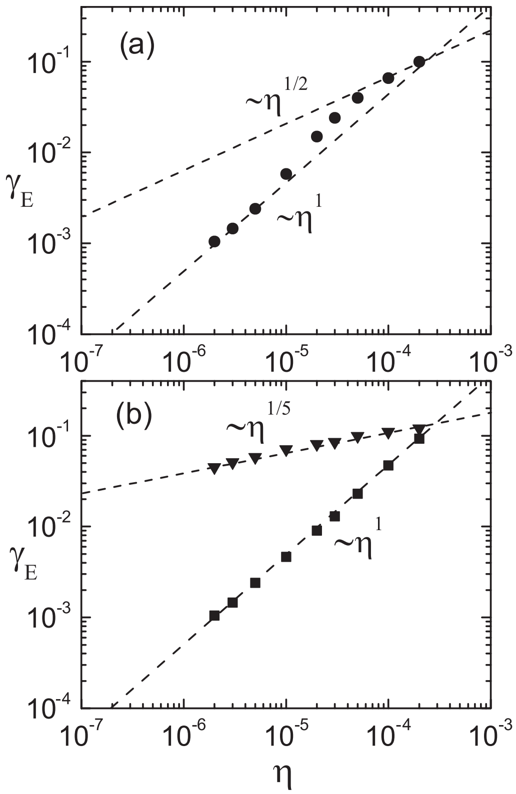

FIG. 2. The growth rate γ_E of plasma kinetic energy and its scaling on resistivity (a) the early nonlinear phase, in dots (b) the second and third nonlinear phases, in triangles and squares, respectively.

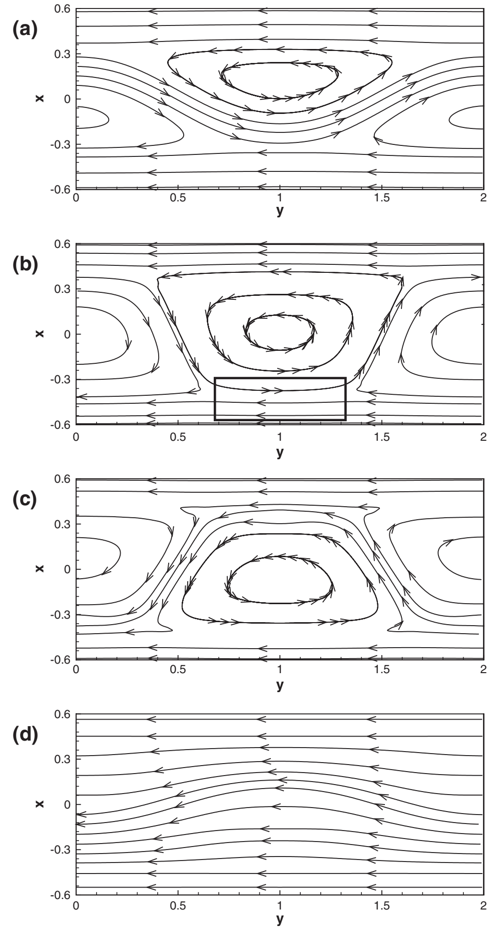

FIG. 3. The magnetic configuration at (a) $t = 184$, (b) $t = 202$, (c) $t = 210$, and (d) $t = 280$, respectively.

In the fast growth phase, however, the growth rate seems almost independent of the plasma resistivity [24]. Nevertheless, by fitting growth rates in a broad range of resistivity, it then obviously obeys a $\eta^{1/5}$ scale, shown in Fig. 2(b).

In order to understand the physical mechanism for the fast growth, we analyze the mode development in Fig. 3, following the structure evolution of the magnetic field lines at four different moments. It has to be pointed out again that there are two resonant surfaces at $x = \pm x_s = \pm 0.25$, and, therefore, as seen in Fig. 3(a), there are two magnetic separatrices formed, one being generated by the upper X point and the other by the lower. The upper (lower) magnetic island in the middle (on the sides) of Fig. 3(a) is formed by reconnection starting at the upper (lower) resonant surface. In the early and transition stages, the two separatrices are separated by the open field lines in between the two islands, seen in Fig. 3(a). As the islands grow bigger, shown in Fig. 3(b), the lower branch of the separatrix of the upper island and the upper branch of the separatrix of the lower island just merge together. In the other words, the edges of the two islands in between the resonant surfaces are overlapped. Thus, as shown in Figs. 3(b) and 3(c), the newly reconnected field lines ejected to the island will reconnect again at the other X point. Focusing ourselves on the small box surrounding the lower X point [Fig. 3(b)], we can find that reconnection at the upper X point generates flux onto the upper boundary of the area surrounded to provide an inward boundary flow to drive reconnection at the lower X point. Because of the symmetry, the same process occurs at the upper X point. Clearly, the process is the same as the inward flow boundary driven reconnection studied previously, with a fast $\eta^{1/5}$ scale growth [29]. Also shown in Fig. 3(c), the upper part of the upper island shrinks in the y direction as reconnection goes on to push the whole structure of the island downward while the lower island is pushed upward. Eventually, the adjacent magnetic islands exchange their relative positions in the x direction, until all field lines between the resonant surfaces reconnected.

Shown in Fig. 4 is the two-dimensional profile of the plasma current at $t = 184$, just before the fast growth phase. It is clearly seen that there are very sharp current peaks in the vicinity of the X points. The current peaks spread in the y direction to extend to current sheets, leading to the island position exchange shown in Fig. 3(c). When the width of the reconnection region in the y direction is

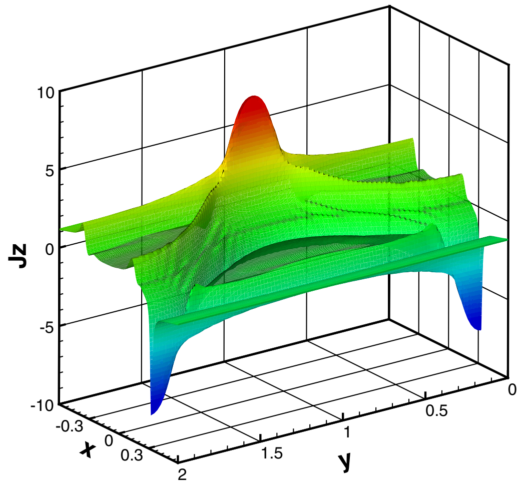

FIG. 4 (color online). The profile of the current density J_Z at $t = 184$.

shortest, the profile of the current forms a current point as described in Ref. [24].

The simulation run for the $m/n = 2/1$ mode shows similar results. Also, the above analysis for the reconnection process of the double tearing mode can also be extended to reconnection in plasmas with multiresonant surfaces, or equivalently multicurrent layers. In general, the magnetic field, or its reconnecting component, changes sign across a resonant surface. Therefore, the magnetic field in the outmost regions outside of the resonant surfaces will have the same direction if there are even numbers of resonant surfaces. In such systems, the field lines between the resonant surfaces will be completely reconnected as shown for the double tearing mode case. On the other hand, the magnetic field in the outmost regions outside of resonant surfaces will direct oppositely if there are odd numbers of the resonant surfaces. In such systems the reconnection process for the field lines between the resonant surfaces will eventually reach a saturated state with a single magnetic island.

The multiphase nonlinear development of magnetic reconnection of the double tearing modes is studied in the numerical simulations. It starts with the early $\eta^{1/2}$ scale Sweet-Parker phase [15,30,31] followed by the η^1 scale slow Rutherford transition phase [32]. After the separatrices of the magnetic islands merging together, the $\eta^{1/5}$ scale fast growth phase onsets. This fast growth can be understood by the equivalent boundary inward flow drive [29]. Then, the decay phase follows to complete the reconnection process with all field lines between the resonant surfaces reconnected. A general rule in prediction of the final state of magnetic reconnection in multiple-resonant-surface systems is also summarized. It finds that the final reconnected state of the systems with even (or odd) numbers of the resonant surfaces is of approximately parallel magnetic field lines (or the single magnetic island). The prediction can be applied to magnetic fusion, solar, and astrophysical plasmas.

This work is supported by NSFC, Grant Nos. 10575031 and 40390155. One of the authors (X. G. W.) would also like to thank K. P. Foundation of Zhejiang University for the support during his visit to Institute for Fusion Theory and Simulation.

*The corresponding author: xgwang@pku.edu.cn

[1] D. Biskamp, *Magnetic Reconnection in Plasmas* (Cambridge University Press, New York, 2000).
[2] E. Priest and T. Forbes, *Magnetic Reconnection: MHD Theory and Applications* (Cambridge University Press, New York, 2000).
[3] J. Birn *et al.*, Astrophys. J. **541**, 1078 (2000).
[4] A. Lazarian and E. T. Vishniac, Astrophys. J. **517**, 700 (1999).
[5] R. B. Dahlburg and J. T. Karpen, J. Geophys. Res. **100**, 23489 (1995).
[6] D. W. Longcope and I. Klapper, Astrophys. J. **579**, 468 (2002).
[7] M. G. Linton and S. K. Antiochos, Astrophys. J. **581**, 703 (2002).
[8] V. S. Titov *et al.*, Astrophys. J. **582**, 1172 (2003).
[9] K. Kusano *et al.*, Astrophys. J. **610**, 537 (2004); K. Kusano, *ibid.* **631**, 1260 (2005).
[10] D. W. Longcope *et al.*, Astrophys. J. **630**, 596 (2005).
[11] K. Bowers and H. Li, Phys. Rev. Lett. **98**, 035002 (2007).
[12] L. L. Lao *et al.*, Phys. Plasmas **3**, 1951 (1996).
[13] Y. Koide *et al.*, Phys. Rev. Lett. **72**, 3662 (1994).
[14] Z. Chang *et al.*, Phys. Rev. Lett. **77**, 3553 (1996).
[15] P. L. Pritchett *et al.*, Phys. Fluids **23**, 1368 (1980).
[16] L. Ofman, Phys. Fluids B **4**, 2751 (1992).
[17] R. L. Dewar and M. Persson, Phys. Plasmas **1**, 1256 (1994).
[18] E. D. Held *et al.*, Phys. Plasmas **6**, 837 (1999).
[19] Q. Yu and S. Günter, Nucl. Fusion **39**, 487 (1999).
[20] E. Fredrickson *et al.*, Phys. Plasmas **7**, 4112 (2000).
[21] J. Q. Dong *et al.*, Phys. Plasmas **10**, 3151 (2003).
[22] J. Q. Dong *et al.*, Phys. Plasmas **11**, 5673 (2004).
[23] Y. Ishii *et al.*, Phys. Plasmas **7**, 4477 (2000).
[24] Y. Ishii, M. Azumi, and Y. Kishimoto, Phys. Rev. Lett. **89**, 205002 (2002); Phys. Plasmas **10**, 3512 (2003).
[25] Y. Ishii *et al.*, Nucl. Fusion **43**, 539 (2003).
[26] A. Bierwage *et al.*, Phys. Rev. Lett. **94**, 065001 (2005).
[27] A. Bierwage *et al.*, Phys. Plasmas **13**, 032506 (2006).
[28] P. H. Rutherford, Phys. Fluids **16**, 1903 (1973).
[29] X. Wang *et al.*, Phys. Plasmas **3**, 2129 (1996).
[30] F. L. Waelbroeck, Phys. Fluids B **1**, 2372 (1989).
[31] X. Wang and A. Bhattacharjee, Phys. Fluids B **4**, 1795 (1992).
[32] F. L. Waelbroeck, Phys. Rev. Lett. **70**, 3259 (1993).